Oct 17th, 12:00 AM

Evaluation of Bolt-hole Elongation Stiffness for the Stiffness Prediction of Cold-formed Steel Bolted Moment-connections

J. B. P. Lim

D. A. Nethercot

Sixteenth International Specialty Conference on Cold-Formed Steel Structures
Orlando, Florida USA, October 17-18, 2002

EVALUATION OF BOLT-HOLE ELONGATION STIFFNESS FOR THE STIFFNESS PREDICTION OF COLD-FORMED STEEL BOLTED MOMENT-CONNECTIONS

J.B.P. Lim[1] and D.A. Nethercot[2]

Abstract

Cold-formed steel bolted moment-connections cannot be considered as rigid because of localised in-plane elongation of the bolt-holes due to bearing of the bolt-shank against the bolt-hole. To therefore calculate the rotational stiffness of such bolted moment-connections, it is necessary to know the load-extension characteristics of bolt-hole elongation. In this paper, a non-linear large-displacement elasto-plastic finite element idealisation of a plain bolt-shank in bearing against a bolt-hole is presented. Graphs of load against bolt-hole elongation are plotted that show good comparison with laboratory test results. A proposed modification of the results allows for the results of a fully-threaded bolt-shank to be predicted. The bolt-hole elongation stiffness so obtained is the main parameter required for the analysis of cold-formed steel frames that use such bolted moment-connections for the joints.

1 Introduction

The authors have recently described a cold-formed steel portal framing system (Lim and Nethercot (2002)) in which back-to-back cold-formed steel sections were used for the members and the eaves and apex joints were formed through brackets using bolted moment-connections (see Fig.1). Such joints cannot be considered as rigid because of localised in-plane elongation of the bolt-holes due to bearing of the bolt-shank against the bolt-hole. To calculate the rotational stiffness of bolted moment-connections, it is necessary to know the load-extension characteristics of bolt-hole elongation. In this paper, a combination of laboratory tests and finite element analyses will be used to determine these characteristics.

[1] Formerly Research Student in Structural Engineering, University of Nottingham, U.K.
Now Engineer, The Steel Construction Institute, U.K.
[2] Formerly Professor in Civil Engineering, University of Nottingham, U.K.
Now Professor in Civil Engineering, I.C.S.T.M, U.K.

2 Phenomenon of bolt-hole elongation

Bolt-hole elongation is the term used to describe the deformation of the bolt-hole caused by bearing of the bolt-shank against the bolt-hole. The main factors on which the load-extension characteristics of bolt-hole elongation depend are:
(1) the thickness of the cold-formed steel plate
(2) the diameter of the bolt-hole
(3) the material properties of the cold-formed steel plate
(4) the diameter of the bolt
(5) the material properties of the bolt
(6) whether the bolt-shank is plain or threaded

3 Literature review

Experimental investigations have been described by Winter (1946), Dhalla *et al* (1971), Chong and Matlock (1975), Gilchrist and Chong (1979) and Zadanfarrokh (1991) and Zadanfarrokh and Bryan (1992). These investigations were mainly concerned with the ultimate load that a single-shear bolted lap-joint could be designed to carry and the effect of the end-distance behind the bolt-hole.

Of these experimental investigations, the most comprehensive was that conducted by Zadanfarrokh and Bryan. Zadanfarrokh and Bryan proposed a semi-empirical design formula that could be used to predict the ultimate load that a single-shear bolted lap-joint could be designed to carry; this design formula has subsequently been adopted by Eurocode No 3 (1996): Part 1 Annex A. Furthermore, unlike the other experimental investigations, Zadanfarrokh and Bryan also measured the flexibility of single-shear bolted lap-joints. This flexibility for single-shear bolted lap-joints is due to both bolt-hole elongation and to bolt-tilt.

However, the bolts used in the eaves and apex joints of Fig.1 are in double shear for which bolt-tilt is prevented owing to symmetry. For both the strength and stiffness design of double-shear bolted lap-joints, the design formula proposed by Zadanfarrokh and Bryan for single-shear bolted lap-joints can be expected to be conservative if applied. In this paper, the load-extension characteristics of bolt-hole elongation of double-shear bolted lap-joints will be determined.

4 Finite element idealisation of plate

The finite element program ABAQUS (Hibbit, Karlsson and Sorensen, Inc. (1995)) will be used to model the plate and simulate contact between the bolt-shank and the bolt-hole. The model will be solved using non-linear large-displacement elasto-plastic analysis.

Details of the finite element idealisation of the plate with a bolt-hole are shown in Fig.2. The plate is of thickness 3mm. The stress-strain relationship of the plate is elastic-perfectly-plastic with a Young's modulus of 205N/mm^2 and a yield stress of 280N/mm^2. By not considering strain hardening, the results can be considered to be conservative.

The plate is modelled using the 20-noded solid element C3D20R. Four elements are used through the thickness of the plate (so that yielding through the thickness of the plate can be simulated) and 40 elements around the bolt-hole. Owing to symmetry, only half the plate is modelled. Lateral displacement is prevented by lateral restraints on the nodes lying on the mid-plane of the plate.

5 Various methods of idealising bearing contact of bolt-shank against bolt-hole

In this Section three methods of idealising the bearing contact of the bolt-shank against the bolt-hole are described.

5.1.1 Method A: effect of bolt-shank represented by constraint equation

Constraint equations can simulate the effect of the bolt-shank on the bolt-hole by permitting only circumferential movement of the nodes around the bolt-hole. In such an idealisation, the bolt-shank is assumed to be rigid. Fig.3(a) shows the direction of the nodal constraints imposed by the constraint equations on the nodes around the bolt-hole. It should be noted that the idealisation of the bearing contact of the bolt-shank against the bolt-hole using Method A is therefore not a contact problem.

It should be recognised that the constraint equation method can only be used for perfect-fit bolt-holes. Also, the results predicted using constraint equations are only valid for predicting the initial bolt-hole elongation stiffness k_b. This is because the direction of each nodal constraint, defined by the constraint equations, is based on initial geometry and is not modified for changes in geometry as the bolt-hole deforms around the bolt-shank. For large deformations of the bolt-hole, the constraint equation method will therefore result in an oddly shaped deformation of the bolt-hole as shown in Fig.3(b); as can be seen, the direction of the nodal constraints in Fig.3(b) are unchanged from Fig.3(a) and so the results predicted using Method A for large-deformations behaviour cannot be accurate.

5.1.2 Method B: effect of bolt-shank represented by rigid body

Fig.4 shows details of the idealisation of the bearing contact of the bolt-shank against the bolt-hole using Method B. As can be seen, the bolt-shank is idealised by a rigid cylindrical body. The

CONTACT PAIRS command is used to define contact between the bolt-shank and the bolt-hole. It should be noted that CONTACT PAIRS are different from contact elements for which a contact stiffness is also required to be defined. The CONTACT PAIRS command is used between pairs of contacting surfaces to prevent the nodes on one surface from penetrating into elements of the opposing surface.

As the contact geometry is defined, Method B does not suffer from the limitation of Method A and the results should be valid for large deformations of the bolt-hole.

5.1.3 Method C: effect of bolt-shank represented by solid body

Fig.5 shows details of idealisation of the bearing contact of the bolt-shank against the bolt-hole using Method C. The bolt-shank is modelled as well as the plate using the same 20-noded solid element C3D20R. The number of elements used around the circumference of the bolt-shank is the same as the number of elements used around the circumference of the bolt-hole. The CONTACT PAIRS command is again used to define contact between the bolt-shank and the bolt-hole.

The total length of the bolt-shank modelled is five times the thickness of the plate. The thickness of each element used for the bolt-shank is the same as that of the plate; 20 elements are therefore used along the length of the bolt-shank.

The stress-strain material relationship of the bolt-shank is elastic-perfectly-plastic with a yield stress of 280N/mm^2. The same value of Young's modulus of the plate is used for the bolt-shank.

In addition to the symmetry constraint conditions imposed on the plate, symmetry constraint conditions are also applied to the bolt-shank. As in the case of the plate, lateral displacement of the bolt-shank is prevented by lateral restraints acting on the nodes lying on the mid-plane of the bolt-shank.

6 Application to perfect-fit bolt-holes

Fig.6 compares, for a perfect-fit bolt-hole, the variation of load against bolt-hole elongation using each of the three methods of idealising the bearing contact between the bolt-shank and the bolt-hole.

The shape of the load-extension curves of bolt-hole elongation can be seen to be bi-linear with an initial stiffness, to be referred to as the bolt-hole elongation stiffness k_b, followed by a secondary stiffness.

It can be seen from Fig.6 that there is good agreement between all three methods for predicting k_b. However, the secondary stiffness predicted by both Methods B and C is slightly higher than

that predicted by Method A. The lower secondary stiffness predicted by Method A is due to the fact that at such large deformations of the bolt-hole, the nodal constraints acting around the bolt-hole cannot totally prevent movement in the direction of the applied load, as the direction of the nodal constraints do not change as the bolt-hole deforms (see sub-section 5.1.1).

It should be appreciated that the modelling of contact is a complex problem. Therefore, the fact that the initial results of both Methods B and C, which use CONTACT PAIRS, are similar to those of Method A indicates that contact has been defined correctly between the bolt-shank and the bolt-hole for Methods B and C. The initial results of Method A can be considered as a benchmark for the initial results of Methods B and C as contact is not defined for Method A.

From Fig.6 it can also be seen that there is very little difference in the results predicted for Methods B and C. The assumption made in Methods A and B that the bolt-shank can be assumed to be rigid is therefore justified. Thus, Method B will be adopted for the results presented in the remainder of this Section.

Fig.7 shows the variation of load against bolt-hole deformation predicted using Method B for different diameters of bolt-shank. As expected, the load at which the stiffness changes from k_b to the secondary stiffness increases with the diameter of the bolt-shank.

For perfect-fit bolt-holes, the results shown in Fig.7 can be used to select the diameter of the bolt that should be used for connections. For examples, if the load that the bolt is required to transmit is known, Fig.7 can be used to select the diameter of the bolt so as to ensure that bolt-hole elongation is small.

7 Application to clearance bolt-holes

7.1.1 Preamble

In the previous Section it was shown that the three methods of idealising the bearing contact between the bolt-shank and the bolt-hole predict similar load-extension characteristics of bolt-hole elongation for perfect-fit bolt-holes. However, only Methods B and C will now be applied to clearance bolt-holes as by its nature Method A cannot be applied to such bolt-holes.

7.1.2 Comparison between Methods B and C

Fig.8 compares the variation of load against bolt-hole elongation using Methods B and C for a 16mm bolt-shank in bearing against an 18mm bolt-hole.

It can be seen that, unlike the case of perfect-fit bolt-holes, the results predicted using Methods B and C are not similar. Firstly, the value of k_b predicted using Method C is significantly higher than that predicted using Method B. Secondly, the variation of load against bolt-hole elongation predicted using Method C is less smooth than the curve predicted using Method B, and also than those for perfect-fit bolt-holes using both Methods B and C. The undulations observed in the results using Method C cannot be explained physically.

In an attempt to improve the load-extension characteristics of bolt-hole elongation predicted using Method C, analyses were conducted using a more refined mesh of both the plate and bolt-shank. No improvement in the results was obtained. Analyses were also conducted using 8-noded instead of 20-noded solid elements for the plate and bolt-shank to ensure that the undulations were not due to the higher stiffness of the mid-side nodes compared to that of the side nodes of quadratic elements. Again, undulations were observed in the results.

Before a reason is suggested for the differences between the load-extension characteristics predicted using Methods B and C, it should first be recalled that in the case of Method B the bolt-shank is not idealised using elements but as a cylindrical rigid-body. As a result, element-to-element contact is not required to be defined for Method B unlike the case for Method C.

It is suggested here that the undulations seen in the load-extension characteristics predicted using Method C can be attributed to difficulties within the ABAQUS algorithm in defining element-to-element contact. It is well known in the field of contact problems that difficulties within the contact algorithm are characterised by undulations in the results and experienced when:
(1) the contacting surfaces are curved and are of different radii
(2) there is large relative sliding between elements of the contacting surfaces
(3) the normal of the contacting surfaces are in different directions
The reasons listed above could therefore explain why undulations were not observed for the case of the perfect-fit bolt-holes using Method C.

Method B gave no such undulations as element-to-element contact is not modelled. For this reason, Method B will be adopted exclusively for the results presented in the remainder of this paper.

7.1.3 Effect of clearance bolt-hole size

Fig.9 shows the variation of load against bolt-hole elongation for varying clearance bolt-hole sizes. It can be seen that there is a large difference between the perfect-fit bolt-hole of 16mm and the same size bolt-shank in a 17mm diameter bolt-hole. However, there is less difference between the other results when the diameter of the clearance hole is greater than 17mm..

Fig.10 shows the effect of the clearance size on the bolt-hole elongation stiffness k_b. It can be seen that the value of k_b is very sensitive to the clearance size when the clearance is small. For values of bolt-hole diameter greater than, say, 17mm it can be seen that k_b is not so sensitive to the diameter of the bolt-hole.

7.1.4 Effect of different bolt diameters

Fig.11 shows the variation of load against bolt-hole elongation for 2mm clearance bolt-holes for bolts of diameters ranging from 8mm to 18mm. The results should be compared against the results shown in Fig.7 for perfect-fit bolt-holes. It can be seen that the effect of clearance bolt-holes is that the initial bolt-hole elongation stiffness k_b is no longer constant but different for each bolt-hole diameter as well as being significantly less. It can also be seen that the results are no longer bi-linear.

8 Laboratory tests

8.1.1 Details of model

Details of the test specimen are shown in Fig.12. The plate is of thickness 3mm, width 100mm and length 340mm. The end distance measured from the centre of the bolt-hole to the edge of the plate is 80mm. The nominal diameter of the bolt-shank and bolt-hole are 16mm and 18mm, respectively.

Details of the experimental set-up to measure bolt-hole elongation are shown in Fig.13. It can be seen that the plate is tested in a double-shear bolted lap-joint arrangement. The thickness of the two outer plates of mild steel is 15.8mm. As this thickness is approximately five times larger than that of the plate under consideration, any elongation of the bolt-holes in the plates of mild steel may be ignored.

The bolt in each test was only finger-tightened; pre-stress was not applied. The double-shear bolted lap-joint test was conducted in a tensile testing machine and the elongation of the bolt-hole was measured using four potentiometers as shown.

The extension rate used was 1mm per minute and data was recorded at the rate of 10 readings per second.

8.1.2 Experimental test results

Four tests were conducted: two tests using plain bolt-shanks and two tests using fully-threaded bolt-shanks. The two tests using plain bolt-shanks will be referred to as test reference P1 and P2. Similarly, the two tests using fully-threaded bolt-shanks will be referred to as test reference T1 and T2. The measured dimensions of the test specimens are summarised in Table 1.

Fig.14 shows the 'engineering' stress-strain curve measured experimentally from tensile coupon tests with the calculated 'true' stress-strain curve superimposed. Table 2 summarises the yield and ultimate stresses of the coupons for both 'engineering' and 'true' stress.

Fig.15 shows the experimentally measured variation of load against bolt-hole elongation while the ultimate load for each test is also given in Table 1. As can be seen, the ultimate load of all four tests are similar. However, the bolt-hole elongation stiffness k_b for the fully-threaded bolt-shank is significantly lower than that for the plain bolt-shank.

9 Comparison between experimental and finite element results for plain bolt-shank case

Two material models of the 'true' stress-strain relationship of the plate will be considered in the finite element analysis as shown in Fig.16. In the first material model (MM1), the stress-strain relationship is assumed to be perfectly plastic after the ultimate stress is reached. In the second material model (MM2), the stress-strain relationship is assumed to continue to strain harden.

Fig.17 compares for test reference P1 the experimental results with the finite element results based on MM1 and MM2. Fig.18 compares the same results for test reference P2.

The finite element results based on MM1 is lower than the experimental results. This is to be expected because as MM1 makes the conservative assumption of a perfectly plastic stress-strain curve after the ultimate tensile stress has been reached. On the other hand, the finite element results obtained using MM2 are higher than the experimental results. Again this is to be expected because the stress-strain relationship used by MM2 is assumed to strain-harden indefinitely without failure due to shear fracture.

However, as can be seen in Fig.18, there is good agreement between the experimental results and both finite element results for bolt-hole elongations of less than 1mm. Either MM1 or MM2 can therefore be used to predict the bolt-hole elongation stiffness k_b.

10 Effect of threads on bolt-hole elongation

The effective stress area A_{eff} of a nominal fully-threaded 16mm diameter bolt is

$$A_{eff} = 157\text{mm}^2$$

from which the effective radius is

$$r_{eff} = \sqrt{\frac{A_{eff}}{\pi}} = 7.07\text{mm}$$

The difference between the nominal radius of 8mm and the effective radius is therefore the effective depth of thread

$$d_{eff} = r_{nom} - r_{eff} = 0.93mm$$

Fig.19 shows the experimental results of load against bolt-hole elongation for the fully-threaded bolt-shank. The finite element result for a plain bolt-shank of diameter 14.14mm, offset by 0.93mm is also superimposed on the same graph. It should be noted that the finite element results are obtained using MM2, as opposed to MM1, as the results predicted using MM2 were shown to be more similar to laboratory test results for the case of the plain bolt-shank described in the previous Section.

It can be seen that after applying the offset of 0.93mm, there is a remarkably close agreement between the variation of load against bolt-hole elongation of the two curves. Therefore, the difference in the initial behaviour of the plain bolt-shank and the fully-threaded bolt-shank may be explained by the fact that the thread initially penetrates into material around the bolt-hole.

11 Proposed bolt-hole elongation for fully-threaded bolts

The finite element model has been shown to be suitable for predicting the initial bolt-hole elongation stiffness k_b for the case plain bolt-shank. The difference between the plain bolt-shank and the fully-threaded bolt-shank was discussed in the previous Section where it was suggested that the thread initially penetrates into material around the bolt-hole.

In the frame analyses described by Lim and Nethercot (2002), the load-extension characteristics of bolt-hole elongation is required for the bearing of a nominal 16mm fully-threaded bolt-shank against a nominal 18mm diameter hole in a plate of nominal thickness 3mm. The stress-strain relationship of the plate is assumed to be elastic-perfectly-plastic with a nominal yield stress of $280N/mm^2$.

It is proposed that the finite element results for a plain bolt-shank are used to predict the variation of load against bolt-hole elongation for bearing against a fully-threaded bolt-shank.

Fig.20 shows the proposed load-extension characteristics for the case of a fully-threaded bolt-shank. As can be seen, the proposed variation of load against bolt-hole elongation is obtained by offsetting the results for bearing against a plain bolt-shank of diameter 14.14mm by the nominal depth of the thread of 0.93mm.

From Fig.20, the initial bolt-hole elongation stiffness k_b of the proposed load-extension characteristics for the case of the fully-threaded bolt-shank is found to be 10.58kN/mm. This is the value of k_b used by the authors in the analysis of a cold-formed steel portal frame (Lim and Nethercot (2002)).

12 Concluding remarks

Three finite element methods of modelling a bolted connection in double shear have been presented and the ability of each method to adequately represent all important features examined. Of the three methods for idealising the contact between the bolt-shank and the bolt-hole Method B, in which the bolt-shank is idealised by a rigid cylindrical body, has been selected as being the most appropriate and has been shown to have good correlation when compared to laboratory test results for a 16mm plain bolt-shank in bearing against an 18mm bolt-hole of a 3mm thick plate. A proposed modification of the results obtained using Method B also allows for the results of a fully-threaded bolt-shank to predicted.

The initial bolt-hole elongation stiffness k_b is predicted using the proposed modification for the bearing of a nominal 16mm fully-threaded bolt-shank against a nominal 18mm diameter hole in a plate of nominal thickness 3mm. This value of k_b is found to be 10.58kN/mm and was used by the authors (Lim and Nethercot (2002)) as part of the procedure to calculate frame deflections of a cold-formed steel portal frame.

Appendix I - References

Chong, K.P. and Matlock, R.B. (1975): 'Light-gauge steel bolted connections without washers', J. Struct. Div., Am. Soc. Civ. Engrs, 101, p1381.

Dhalla, A.K., Samuel, J.E. and Winter, G. (1971): 'Connections in thin low ductility steels', J. Struct. Div., Am. Soc. Civ. Engrs, 97, p2549.

Eurocode 3 (1996): Design of steel structures: Part 1 - General rules and rules for buildings, Brussels, Committee European de Normalisation.

Hibbit, Karlsson and Sorensen, Inc. (1995a): ABAQUS Theory Manual, Hibbitt, Karlsson and Sorensen, Inc.

Lim, J. and Nethercot, D.A. (2002): 'Design and development of a general cold-formed steel portal framing system', accepted for publication in The Structural Engineer.

Winter, G. (1946): 'Tests on bolted connections in light gauge steel', Trans. Am. Soc. Civ. Engrs, 112, p527.

Zadanfarrokh, F. (1991): Analysis and design of bolted connections in cold-formed steel members, PhD thesis, University of Salford.

Zadanfarrokh, F. and Bryan, E.R. (1992): 'Testing and design of bolted connections in cold formed steel sections', Proc. 11th International Speciality Conference on Cold-formed Steel Structures, St Louis, University of Missouri-Rolla, p625.

Appendix II - Notation

t	thickness of plate
k_b	bolt-hole elongation stiffness
d_b	diameter of bolt
d_h	diameter of bolt-hole
d_e	end distance measured from centre of bolt-hole
σ_{ult}	ultimate stress
σ_y	yield stress

Table 1 Properties of plate and bolt-shank used in laboratory tests, and results of ultimate load

Test reference	Plain /threaded	t (mm)	d_h (mm)	d_b (mm)	end distance (mm)	P_{ult} (kN)
P1	plain	2.989	17.70	15.58	79.95	94.00
P2	plain	2.977	17.65	15.75	79.29	91.00
T1	threaded	2.954	17.80	15.81	79.54	91.60
T2	threaded	2.984	17.69	15.71	79.51	87.40

Table 2 Material properties of plate used in laboratory tests

Type of stress measurement	σ_y (N/mm^2)	σ_u (N/mm^2)
'Engineering'	343	431
'True'	344	474

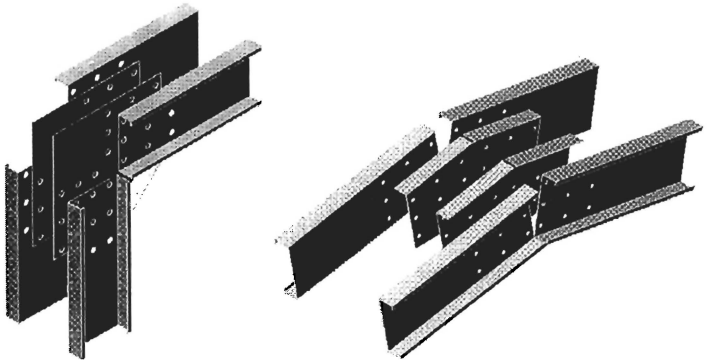

(a) Eaves joint (b) Apex joint

Fig.1 Details of joints of proposed cold-formed steel portal framing system

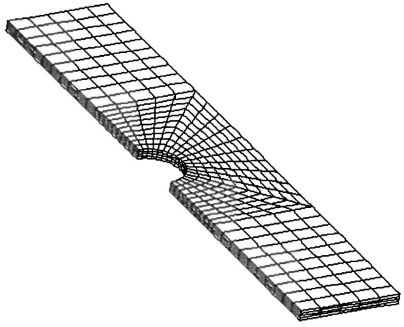

Fig.2 Details of finite element mesh of plate with bolt-hole

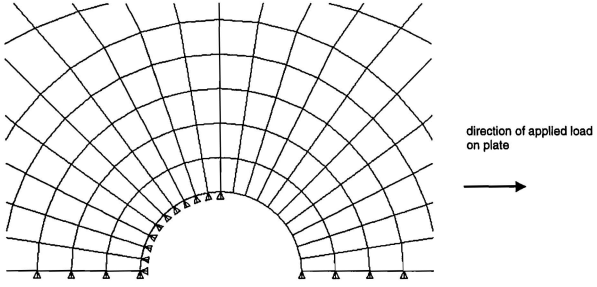

(a) Direction of nodal constraints imposed on nodes around bolt-hole

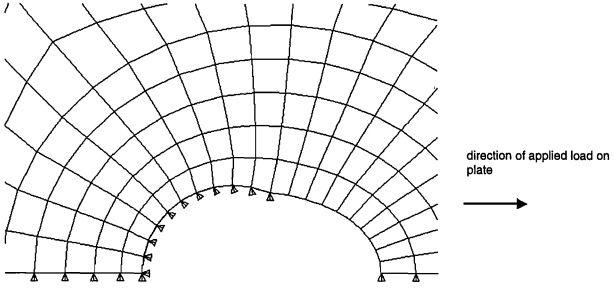

(b) Deformed shape of bolt-hole

Fig.3 Details of finite element mesh of plate with bolt-hole based on Method A

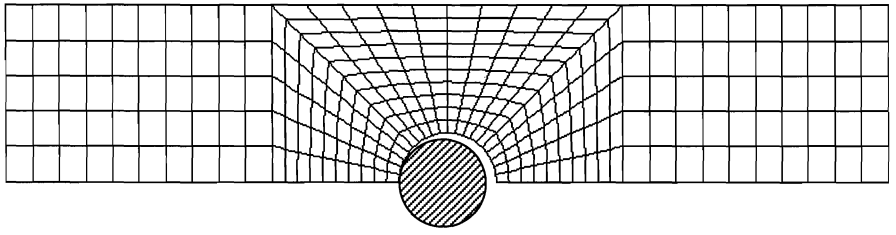

Fig.4 Details of finite element mesh of plate and rigid bolt-shank based on Method B

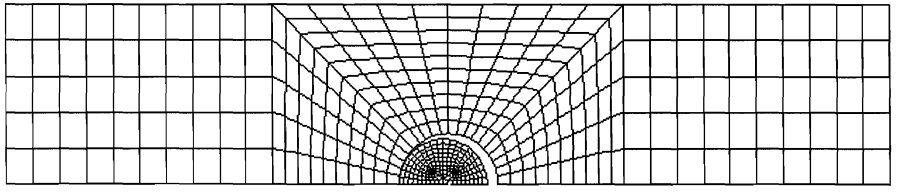

Fig.5 Details of finite element mesh of plate and non-rigid bolt-shank based on Method C

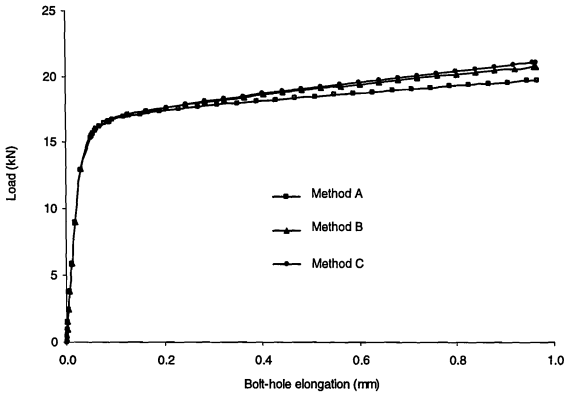

Fig.6 Comparison of results using various methods of idealising bolt-shank for a perfect-fit bolt-hole

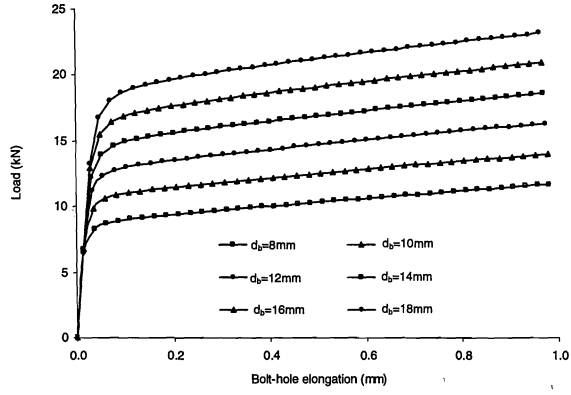

Fig.7 Variation of load against bolt-hole elongation for perfect-fit bolts of different diameter. Results obtained using Method B

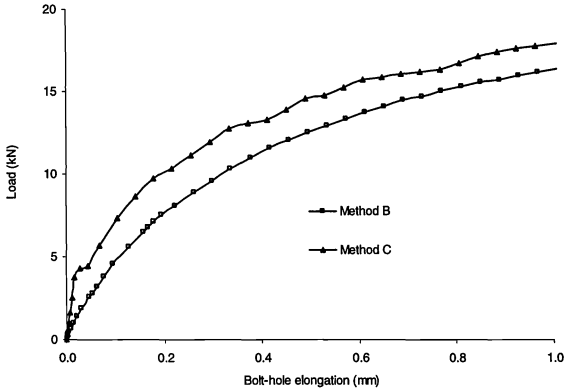

Fig.8 Comparison of results between Methods B and C for 16mm bolt-shank in bearing against 18mm bolt-hole

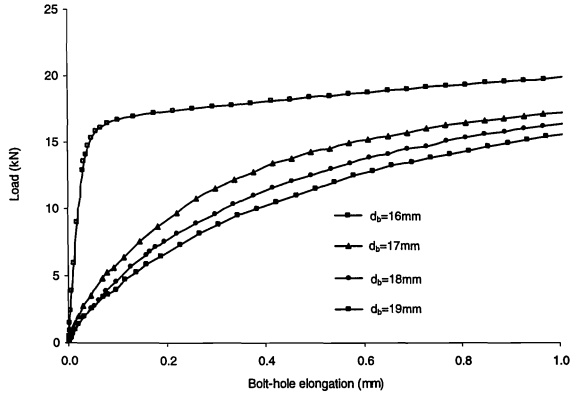

Fig.9 Variation of load against bolt-hole elongation for 16mm bolt-shank in bearing against clearance bolt-holes of varying sizes

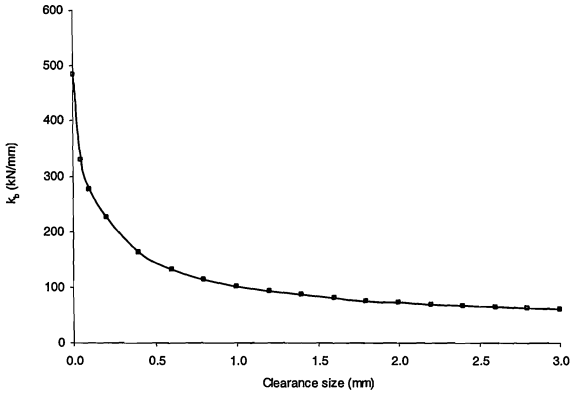

Fig.10 Variation of bolt-hole elongation stiffness k_b against size of clearance bolt-hole

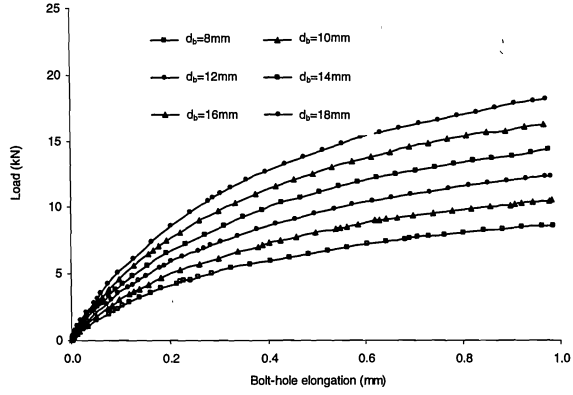

Fig.11 Variation of load against bolt-hole elongation for various bolt sizes with 2mm clearance bolt-hole

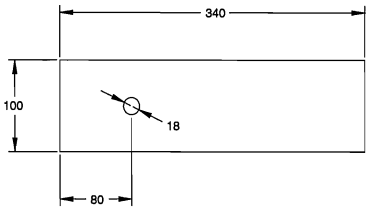

Fig.12 Details of plate with bolt-hole

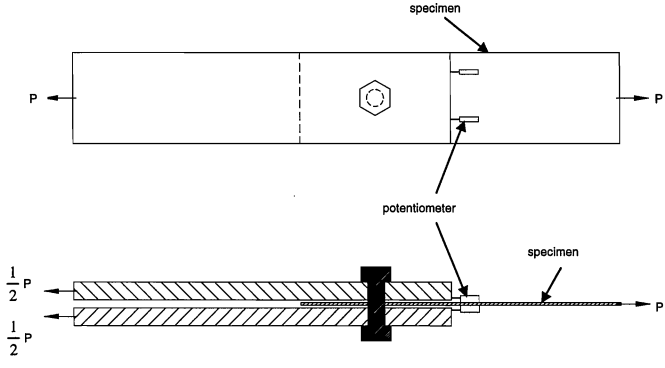

Fig.13 Laboratory test set-up to measure bolt-hole elongation

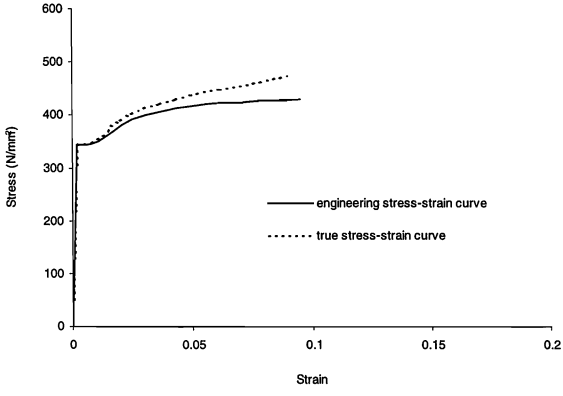

Fig.14 Variation of stress against strain of plate used in experiment to measure bolt-hole elongation

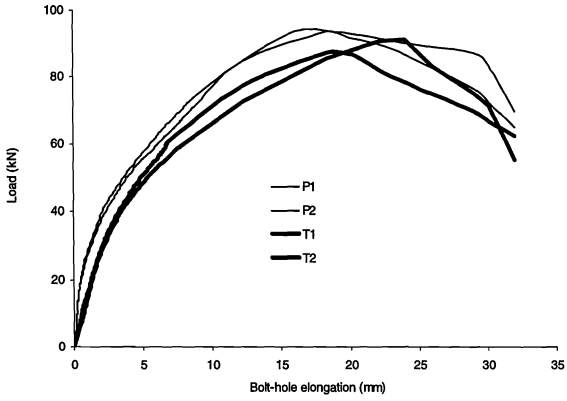

Fig.15 Variation of load against bolt-hole elongation determined experimentally

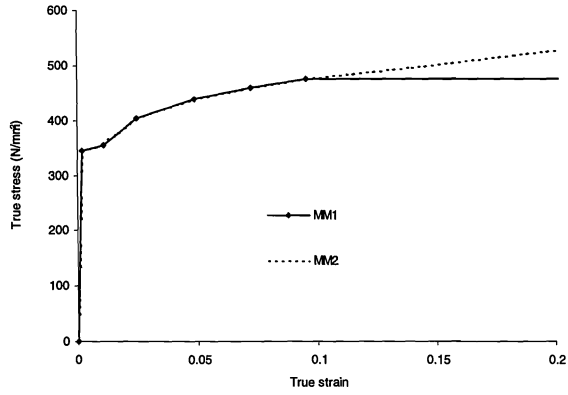

Fig.16 Material models used in finite element analysis to determine bolt-hole elongation

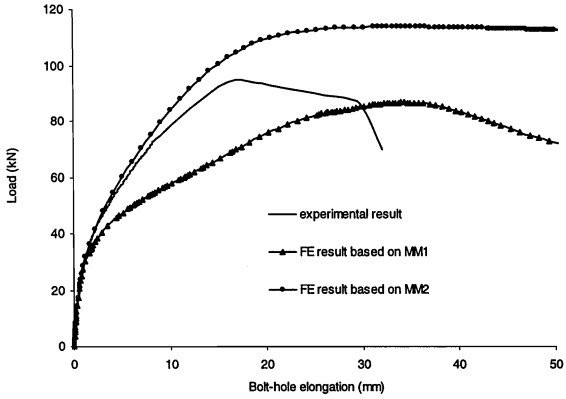

(a) Plot to failure

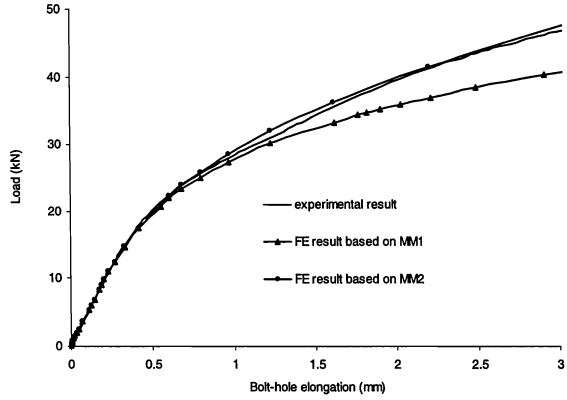

(b) Magnified plot

Fig.17 Comparison between experimental and finite element results for test reference P1

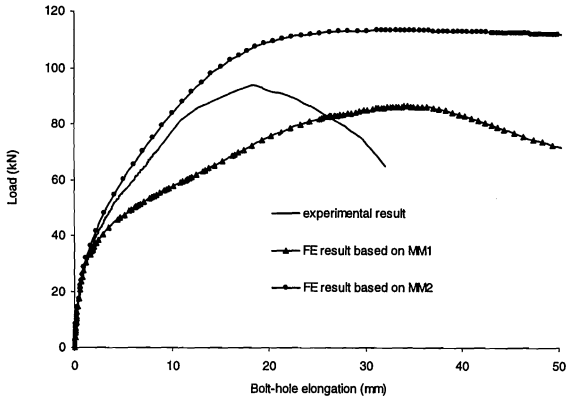

(a) Plot to failure

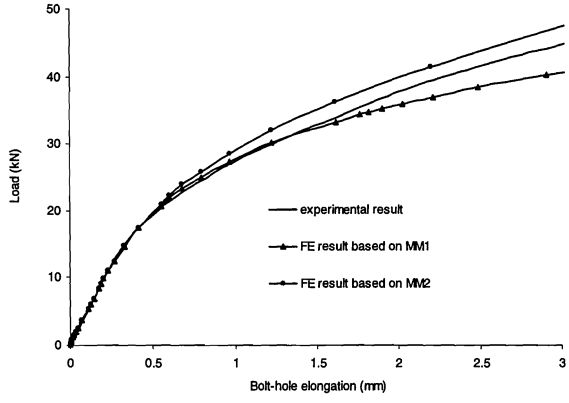

(b) Magnified plot

Fig.18 Comparison between experimental and finite element results for test reference P2

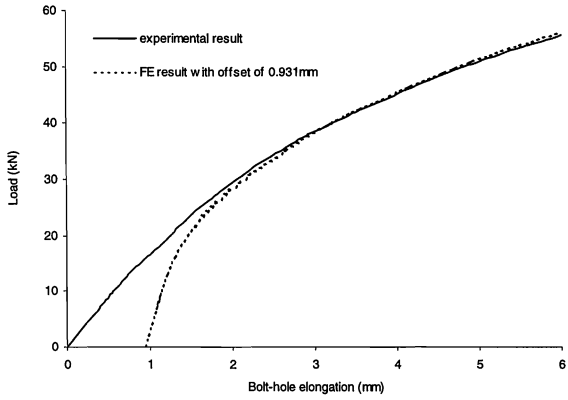

Fig.19 Comparison between experimental and finite element results for test reference T1

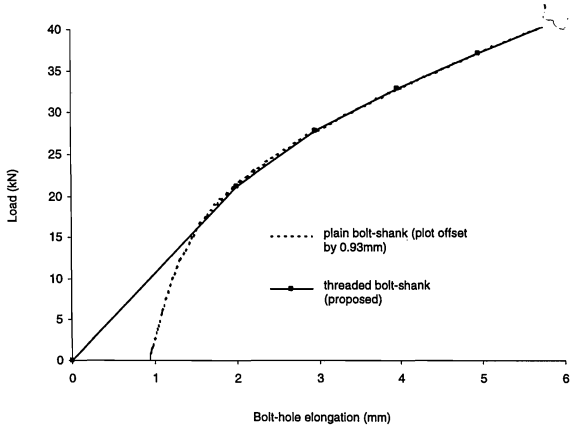

Fig.20 Proposed bolt-hole elongation model for 16mm threaded bolt in bearing against nominal 18mm hole in plate with yield stress of 280N/mm^2